ELSEVIER

Journal of Organometallic Chemistry 551 (1998) 235–246

Journal of Organometallic Chemistry

Construction of unusual cluster geometries about a dicarbon ligand: reactions of $Ru_5(\mu_5\text{-}C_2)(\mu\text{-}SMe)_2(\mu\text{-}PPh_2)_2(CO)_{11}$ with iron or ruthenium carbonyls [1]

Chris J. Adams [a], Michael I. Bruce [a,*], Brian W. Skelton [b], Allan H. White [b]

[a] *Department of Chemistry, University of Adelaide, Adelaide, South Australia 5005, Australia*
[b] *Department of Chemistry, University of Western Australia, Nedlands, Western Australia 6907, Australia*

Received 7 May 1997; received in revised form 10 July 1997

Abstract

The open pentanuclear cluster $Ru_5(\mu_5\text{-}C_2)(\mu\text{-}SMe)_2(\mu\text{-}PPh_2)_2(CO)_{11}$ reacts with iron or ruthenium carbonyls to give a series of higher nuclearity clusters in which the C_2 ligand acts as a template about which the extra metal atoms aggregate. The crystallographically-determined structures of the following four complexes are reported: $MRu_5(\mu_6\text{-}C_2)(\mu\text{-}SMe)_2(\mu\text{-}PPh_2)_2(CO)_{14}$ and $M_2Ru_5(\mu_6\text{-}C_2)(\mu_3\text{-}SMe)_2(\mu\text{-}PPh_2)_2(\mu\text{-}CO)(CO)_{15}$ (M = Fe, Ru). The metal cores of the hexanuclear clusters are constructed of two edge-sharing squares (forming a permetallabicyclo[2.2.0]hexane skeleton), while in the latter, the seventh metal atom bridges an outer edge of one of the squares. Alternatively, the core geometries can be related to the trigonal prism. © 1998 Elsevier Science S.A.

Keywords: Dicarbon ligand; Ruthenium carbonyl; Trigonal prism

1. Introduction

Their potential uses as novel materials with liquid crystal [1] or nonlinear optical properties [2–4], or as one-dimensional molecular wires [5,6], has focused interest on metal complexes containing all-carbon molecules, C_n [7–9]. Several metal cluster complexes that contain the simplest carbon molecule encapsulated by a metal cage have been reported. These include $[Co_6Ni_2(C_2)(CO)_{16}]^{2-}$ [10], $[Co_3Ni_7(C_2)(CO)_{15}]^{3-}$ $[Ni_{10}(C_2)(CO)_{16}]^{2-}$ [11,12] and $Rh_{12}(C_2)_2(CO)_{25}$ [13]. Little chemistry of these systems has been reported, with the exception that treatment of the Co–Ni cluster with H_2 at ambient temperatures afforded ethane, $Ni(CO)_4$ and $[Co(CO)_4]^-$ [12].

A variety of polynuclear systems in which the C_2 ligand is attached to more open clusters is also known. In both $\{Co_3(CO)_9\}_2(\mu_3,\mu_3\text{-}C_2)$ [14–17] and the heterometallic complex $[Fe_3Co_3(CO)_{18}(\mu_3,\mu_3\text{-}C_2)]^{2-}$ [18], the C_2 unit can be considered to be a carbon-linked bis-methylidyne system. Other examples include $Co_6(\mu_6\text{-}C_2)(\mu_4\text{-}S)(CO)_{14}$ [19], $FeRu_6(\mu_5\text{-}C_2)(\mu_5\text{-}C_2H)(CO)_{16}$ [20] and $FeRu_6(\mu_5\text{-}C_2)_2(CO)_{17}(\eta\text{-}C_5Me_5)_2$ [21].

Several years ago, we described the synthesis of the open pentanuclear cluster $Ru_5(\mu_5\text{-}C_2)(\mu\text{-}SMe)_2(\mu\text{-}PPh_2)_2(CO)_{11}$ (**1**), which contains an exposed C_2 ligand sitting atop a somewhat distorted pentagon of ruthenium atoms [22]. The multisite bonding capabilities of the C_2 ligand have obvious consequences on its reactivity, and the extensive chemistry of **1** has been described elsewhere [23,24]. The designed build-up of clusters with novel architectures is an interesting exercise. We decided to make use of the potential ability of the μ-SMe groups present in **1** to expand their coordination to μ_3 as an aid the incorporation of extra metal atoms into the Ru_5 cluster of **1** and its use as a precursor to higher nuclearity clusters built up around the C_2 ligand has been communicated briefly [25]. Herein, we describe

---

[*] Corresponding author.

[1] Dedicated to Peter Maitlis, outstanding chemist and colleague, in recognition of his unparalleled contributions to organometallic chemistry.

the complexes that we have obtained from reactions between **1** and $Fe_2(CO)_9$ or $Ru(CO)_5$.

2. Results

Reactions between **1** and $Fe_2(CO)_9$ or $Ru(CO)_5$ were carried out in toluene in sealed tubes at about 100°C for periods of up to 6 h. Conventional work-up using preparative thin-layer chromatography afforded intensely coloured bands containing the novel clusters $MRu_5(\mu_6\text{-}C_2)(\mu\text{-SMe})_2(\mu\text{-PPh}_2)_2(CO)_{14}$ [M = Fe (**2**) or Ru (**3**)] and $M_2Ru_5(\mu_6\text{-}C_2)(\mu_3\text{-SMe})_2(\mu\text{-PPh}_2)_2(\mu\text{-CO})_{15}$ [M = Fe (**4**), Ru (**5**)] as crystalline solids with essentially total conversions of **1** (Scheme 1).

2.1. (a) $Ru_5M(\mu_6\text{-}C_2)(\mu\text{-SMe})_2(\mu\text{-PPh}_2)_2(CO)_{14}$ [M = Fe (2) or Ru (3)] [M = Fe (2) or Ru (3)]

The orange hexanuclear complexes **2** and **3** have seven terminal ν(CO) bands in their IR spectra. The ^1H NMR spectra contain the expected resonances for the SMe [at δ 1.87 and 1.93 (**2**), 1.78 (**3**)] and PPh_2 groups [at δ 6.90–7.83 (**2**), 6.79–7.82 (**3**)]. In the ^{13}C NMR, singlets [at δ 18.56 and 18.79 (**2**), 18.69 (**3**)] are assigned to the SMe groups, while the Ph resonances occur as extended multiplets between δ 127 and 143 for both complexes. As shown by the X-ray studies (below), the SMe groups in **2** are chemically inequivalent and give rise to two signals, but in homometallic **3**, they are equivalent. In the CO region, only seven resonances (one broadened) were found between δ 191 and 213 (**2**), while four were observed for **3** between δ 192 and 201. The C_2 ligands, of which both carbons are equivalent in both complexes, give rise to doublets at δ 254.9 (**2**) and 252.2 (**3**). The FAB mass spectra contained M^+ ions at 1442 (**2**) and 1459 ($[M-CO]^+$) (**3**), each of which fragments by loss of up to 14 (**2**) or 13 (**3**) CO groups.

Both complexes were fully characterised by single crystal X-ray structural determinations. As expected, they are isostructural. Figs. 1 and 2 contain views of single molecules of **2** and **3**, respectively, while important bond parameters are given in Table 1. The six-atom metal core consists of two rhomboids sharing an edge, which in **2** consists of a pair of disordered Fe/Ru atoms. The dihedral angles are ~ 83 (**2**) and 82.28(3)°

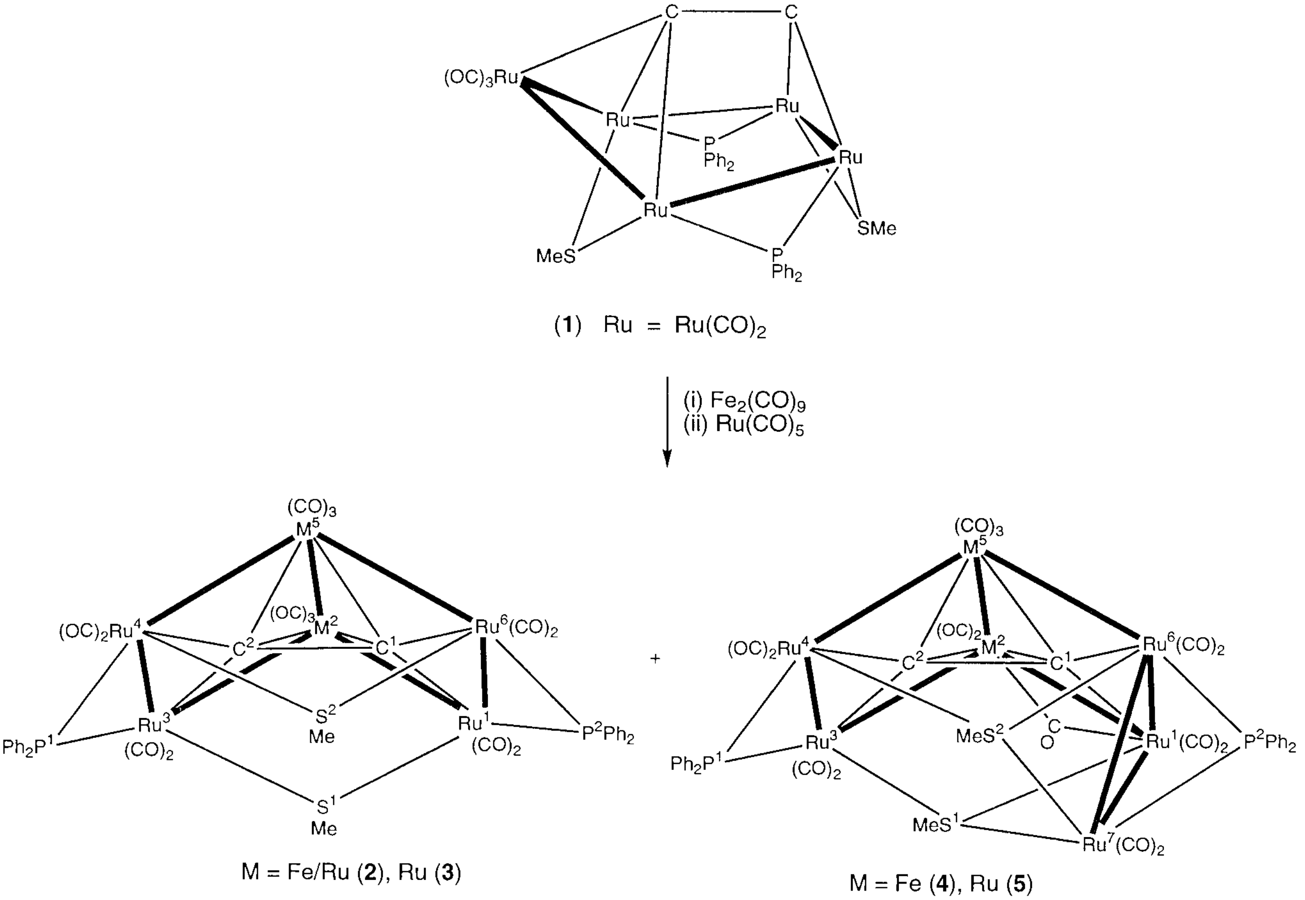

Scheme 1.

(**3**). Each carbon of the μ_4,μ_4-C_2 ligand is approximately under the centre of the rhomboid [C(1) lies ~ 0.38 (**2**), 0.384(7) Å (**3**) from the planes of the M(1,2,5,6) atoms, atom C(2) similarly lies ~ 0.36 (**2**), 0.374(6) Å (**3**) from the M(2,3,4,5) planes], with Fe–C and Ru–C distances between 2.05 and 2.06 Å (Fe) and between 2.081(5) and 2.146(6) Å (Ru). In this respect, the attachment of the carbons to the M_4 rhomboids resemble, although having somewhat longer M–C distances, those found in the bases of carbido complexes such as $M_5C(CO)_{15}$ (M = Fe, Fe–C = 1.89 Å (av.) [26]; Ru, Ru–C = 2.05(3) Å (av.) [27]). However, in **2** and **3**, the two carbon atoms are also bonded to each other [C(1)–C(2) 1.355(9) (**2**), 1.381(8) Å (**3**)], with the C(1)–C(2) vector making angles of ~ 41, 42° (**2**) and 40.67(2), 41.61(2)° (**3**) with the M_4 planes.

The M–M bonds range between 2.86(1) (disordered M...M separation) and 2.97(1) Å (for **2**) and between 2.884(1) and 2.985(1) Å (for **3**); corresponding Ru–Ru bonds in **2** and **3** are of comparable length. The hinge bond M(2)–M(5) is 2.90(1) Å in **2**, this distance being the mean of the two disordered Fe/Ru pairs. In **3**, this Ru–Ru separation is 2.966(1) Å. The 'outer' Ru(1)–Ru(6) and Ru(3)–Ru(4) bonds (which are each bridged by the PPh_2 groups) are 2.899, 2.880(2) Å (**2**) and 2.891, 2.884(1) Å (**3**), while the other M–M separations [2.915–2.97 Å (**2**), 2.954–2.965(1) Å (**3**)] are all somewhat longer. Within the rhomboids, the

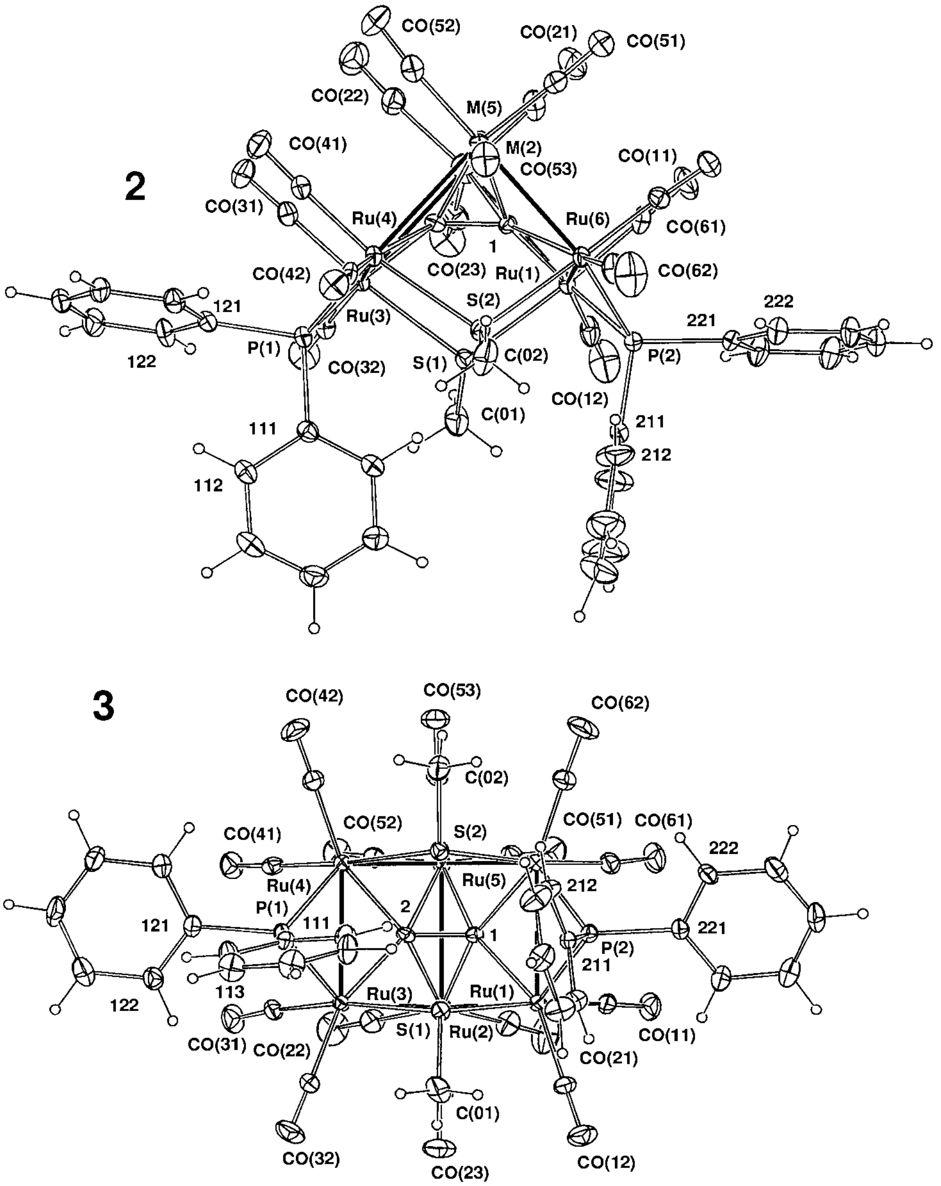

Fig. 1. Molecular projections of (a) **2** in the orientation of Scheme 1, and (b) **3** down the molecular quasi-axis. In this figure and in Fig. 2, 20% probability amplitude thermal ellipsoids are shown for non-hydrogen atoms; hydrogen atoms have arbitrary radii of 0.1 Å.

Ru(1)M(2)M(5)Ru(6) and M(2)Ru(3)Ru(4)M(5) atoms are nearly coplanar (χ^2 359, 93 for **3**). and the dihedral angles between these planes are ∼ 97° (**2**) and 97.72(2)° (**3**).

The Ru–S distances [2.442–2.459(2) Å (**2**); 2.449–2.470(2) Å (**3**)] are similar to others found bridging nonbonding Ru ... Ru vectors, e.g., 2.449, 2.454(1) Å in **1**. The asymmetry is reflected in the nonbonded Ru(1) ... Ru(3) distances [3.877 (2). 3.931(2) Å (**3**)] and the Ru(4) ... Ru(6) separations are 3.924 (2), 3.897(2) Å (**3**). The Ru–P distances [2.294–2.326(3) Å (**2**), 2.298–2.331(2) Å (**3**)] are within the range normally found for bonds to bridging PR_2 groups; the bridges are slightly unsymmetrical. A consistent feature through both structures is the common disposition of the phenyl groups associated with these ligands. Coordination is completed by 14 CO groups, three on each of the hinge atoms and two on each of the other four Ru atoms.

2.2. (b) $M_2Ru_5(\mu_6\text{-}C_2)(\mu_3\text{-}SMe)_2(\mu\text{-}PPh_2)_2(\mu\text{-}CO)(CO)_{15}$ [M = Fe (**4**), Ru) (**5**)]

The black crystalline heptanuclear clusters **4** and **5** have similar spectroscopic properties that are in accord

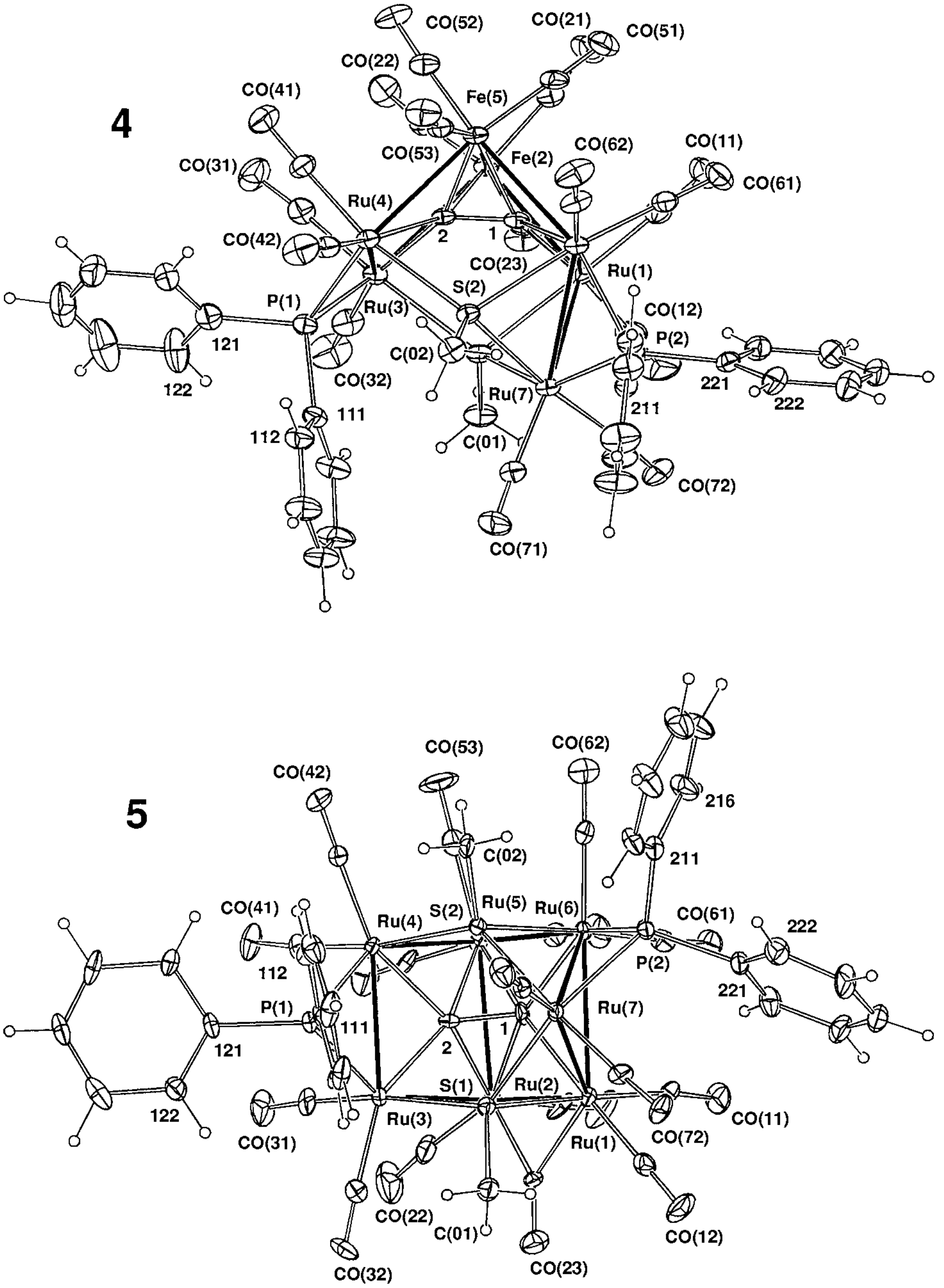

Fig. 2. Molecular projections of (a) **4** in the orientation of Scheme 1 and (b) **5** down the molecular quasi-axis of the M_6 array.

with their solid-state structures (see below). The IR spectra contain many terminal ν(CO) bands and one assigned to a bridging CO group at 1872 (**4**) or 1820 cm^{-1} (**5**). The ^{1}H NMR spectra contain the expected resonances for the SMe groups, at δ 1.70 and 2.85 in **4** and δ 1.58 and 2.79 in **5**. Satisfactory ^{13}C NMR spectra have not yet been obtained. The FAB mass spectra are unexceptional, containing M^{+} ions at m/z 1554 (**4**) and 1644 (**5**), respectively, each of which fragments by loss of up to 16 CO groups.

The molecular structures of **4** and **5** have been confirmed by single-crystal X-ray structural determinations. Plots of the two structures are shown in Figs. 3 and 4, respectively, while significant bond parameters are collected in Table 1. The structures are similar to those of **2** and **3**, the seventh metal atom (Ru in both cases) bridging an edge of one of the square faces (in **4**, the one not involving the iron atom). In **4**, the two iron atoms form the shared edge of the fused squares; these atoms are ruthenium in **5**. In these complexes, the SMe

Table 1
Significant bond parameters for complexes **2**, **3**, **4** and **5**

	2 ($FeRu_5$)	**3** (Ru_6)	**4** (Fe_2Ru_5)	**5** (Ru_7)
Bond distances (Å)				
Ru(1)–M(2)	2.915(9)[a], 2.938(2)	2.954(1)	2.705(1)	2.803(3)
Ru(1)–Ru(6)	2.899(2)	2.891(1)	3.187(1)	3.153(2)
Ru(1)–Ru(7)	–	–	3.054(1)	3.029(2)
M(2)–Ru(3)	2.932(9)[a], 2.944(4)	2.983(1)	2.939(1)	2.977(2)
M(2)–M(5)	2.90(1)[a], 2.908(7)	2.966(1)	2.795(2)	3.008(2)
Ru(3)–Ru(4)	2.880(2)	2.884(1)	2.857(1)	2.840(2)
Ru(4)–M(5)	2.97(1)[a], 2.967(7)	2.979(1)	2.843(1)	2.928(2)
M(5)–Ru(6)	2.92(1)[a], 2.924(7)	2.985(1)	2.881(1)	2.965(3)
Ru(6)–Ru(7)	–	–	2.939(1)	2.976(2)
Ru(1)–S(1)	2.442(2)	2.470(2)	2.409(2)	2.426(4)
Ru(3)–S(1)	2.451(2)	2.468(2)	2.470(2)	2.482(4)
Ru(7)–S(1)	–	–	2.424(2)	2.412(4)
Ru(4)–S(2)	2.454(2)	2.449(2)	2.452(2)	2.453(4)
Ru(6)–S(2)	2.459(2)	2.454(2)	2.417(2)	2.411(4)
Ru(7)–S(2)	–	–	2.454(2)	2.434(4)
Ru(3)–P(1)	2.309(2)	2.312(2)	2.293(2)	2.310(4)
Ru(4)–P(1)	2.326(3)	2.331(2)	2.306(2)	2.303(4)
Ru(1)–P(2)	2.294(2)	2.298(2)	–	–
Ru(6)–P(2)	2.302(2)	2.326(2)	2.335(2)	2.361(4)
Ru(7)–P(2)	–	–	2.314(2)	2.320(4)
Ru(1)–C(1)	2.111(5)	2.095(6)	2.093(7)	2.14(1)
M(2)–C(1)	2.06(1)[a], 2.081(7)	2.117(6)	2.058(6)	2.21(1)
M(5)–C(1)	2.05(1)[a], 2.079(7)	2.131(6)	2.050(6)	2.17(1)
Ru(6)–C(1)	2.119(8)	2.139(6)	2.116(6)	2.09(1)
M(2)–C(2)	2.06(1)[a], 2.081(7)	2.133(6)	1.998(6)	2.13(1)
Ru(3)–C(2)	2.120(6)	2.096(6)	2.104(7)	2.09(1)
Ru(4)–C(2)	2.117(6)	2.111(6)	2.119(7)	2.14(1)
M(5)(–C(2)	2.05(1)[a], 2.080(7)	2.146(6)	2.020(7)	2.13(1)
C(1)–C(2)	1.355(9)	1.381(8)	1.38(1)	1.37(2)
Bond angles (°)				
M(2)–Ru(1)–Ru(6)	89.9(2)*, 90.03(8)	91.57(3)	87.97(4)	89.93(6)
Ru(1)–M(2)–Ru(3)	83.1(2)*, 82.5(1)	82.93(3)	85.49(5)	83.95(6)
Ru(1)–M(2)–Ru(5)	90.3(3)*, 89.7(3)	89.03(3)	95.36(5)	93.07(6)
Ru(3)–M(2)–Ru(5)	90.4(3)*, 90.2(3)	89.09(4)	89.70(5)	86.99(6)
M(2)–Ru(3)–Ru(4)	90.3(2)*, 90.42(9)	90.84(4)	88.36(4)	92.08(6)
Ru(3)–Ru(4)–M(5)	89.3(2)*, 90.1(1)	90.74(4)	90.41(4)	91.13(6)
M(2)–M(5)–Ru(4)	-, 89.4(2)	89.32(4)	91.54(5)	89.75(6)
M(2)–M(5)–Ru(6)	-, 90.1(2)	89.51(3)	92.68(5)	89.80(6)
Ru(4)–M(5)–Ru(6)	83.4(3)*, 83.5(2)	81.61(3)	86.11(5)	83.36(6)
Ru(1)–Ru(6)–M(5)	89.3(2)*, 90.2(1)	89.87(3)	84.01(4)	87.18(6)
Ru(1)–S(1)–Ru(3)	104.82(7)	105.52(7)	103.63(7)	104.0(1)
Ru(1)–S(1)–Ru(7)	–	–		
Ru(3)–S(1)–Ru(7)	–	–	128.63(9)	128.1(2)
Ru(4)–S(2)–Ru(6)	105.98(7)	105.29(7)	106.75(7)	107.3(1)
Ru(4)–S(2)–Ru(7)	–	–	129.77(8)	129.3(2)
Ru(6)–S(2)–Ru(7)	–	–		

[a] Values for Fe components of disordered pairs.

groups are now triple-bridging, atoms Ru(3)S(1)Ru(7)S(2)Ru(4) forming essentially planar pentagons (χ^2 477, 22). The PPh_2 groups bridge the Ru(3)–Ru(4) and Ru(6)–Ru(7) vectors.

Coordination is completed by 15 terminal CO groups, two on each metal atom except M(5), which has three [the expected third CO on M(2) is found bridging the Ru(1)–M(2) vector]. The presence of the latter results in short Ru(1)–M(2) separations [2.705(1) Å (**4**), 2.803(3) Å (**5**)], but the Ru(1)M(2)M(5)Ru(6) rhomboid remains essentially undistorted (χ^2 156, 286). For **4** and **5**, the dihedral angles between the mean M_4 planes are 85.83(3)° and 83.61(4)°, respectively.

As found for **2** and **3**, atoms C(1) and C(2) are 0.363(7), 0.40(2) and 0.398(7), 0.43(1) Å below their respective M_4 planes, with the C(1)–C(2) vector making angles of 44.16(2), 41.69(2) (**4**) and 44.16(3), 39.57(3)° (**5**) with the M_4 planes. The Fe–C distances in **4** are between 1.999(6) and 2.058(6) Å and the Ru–C distances between 2.093(7) and 2.119(7) Å (**4**) and 2.09(1)–2.21(1) Å (**5**). The C(1)–C(2) separations are 1.38(1) Å (**4**) and 1.37(2) Å (**5**), consistent with some C–C multiple bonding character.

Detailed comparisons of the four complexes reveal several significant differences between the MRu_5 and M_2Ru_5 structures. Thus, in the M(2)Ru(3)Ru(4)M(5) rhombus, with the exception of the hinge M(2)–M(5) bond, the three M–M separations are significantly shorter in **5** when compared with **3** [2.977, 2.840, 2.928(2) Å in **5** vs. 2.983, 2.884, 2.979(1) Å in **3**]. Similarly, Ru(1)–Ru(2) and Ru(5)–Ru(6) are 2.954, 2.985(1) Å in **3** and 2.803, 2.965(2) Å in **5**. In contrast, Ru(1)–Ru(6) and Ru(2)–Ru(5) are considerably lengthened in **5**: 3.153, 3.008(2) Å vs 2.891, 2.966(1) Å in **3**. Similar differences are found in **2** and **4** for the Fe(2)–Fe(5) separations, which are 2.795(2) Å in **2** and 3.008(2) Å in **4**. The Ru(7)–Ru(1,6) vectors are also long in both complexes, at 3.054, 2.939(1) Å in **4** and 2.976, 3.029(2) Å in **5**.

3. Discussion

We have shown that the open C_2-containing cluster **1** reacts with $Fe_2(CO)_9$ or $Ru(CO)_5$ to give high yields of six- and seven-atom clusters with novel geometries. The structures of the heteronuclear clusters give some insight into the location of the added metal atoms, which are found within the metal skeleton. A possible route to these complexes is shown in Scheme 2.

We note that calculations of electron density in **1** indicate that it is concentrated both on the C_2 unit and on the SMe group bridging the nonbonded Ru...Ru vector [28]. These two sites would be expected to be those attacked by the entering $M(CO)_n$ fragment or during any cluster rearrangement that might occur during the reaction. In accord with this idea, we propose that an $M(CO)_3$ fragment derived from the carbonyls adds to the C_2 ligand, with concomitant M–M bond formation between other atoms of the Ru_5 pentagon. Addition of the second $M(CO)_3$ fragment occurs similarly, pushing one of the Ru atoms to a position where an Ru–Ru bond is bridged. At the same time, the SMe groups are brought within bonding range of a third Ru

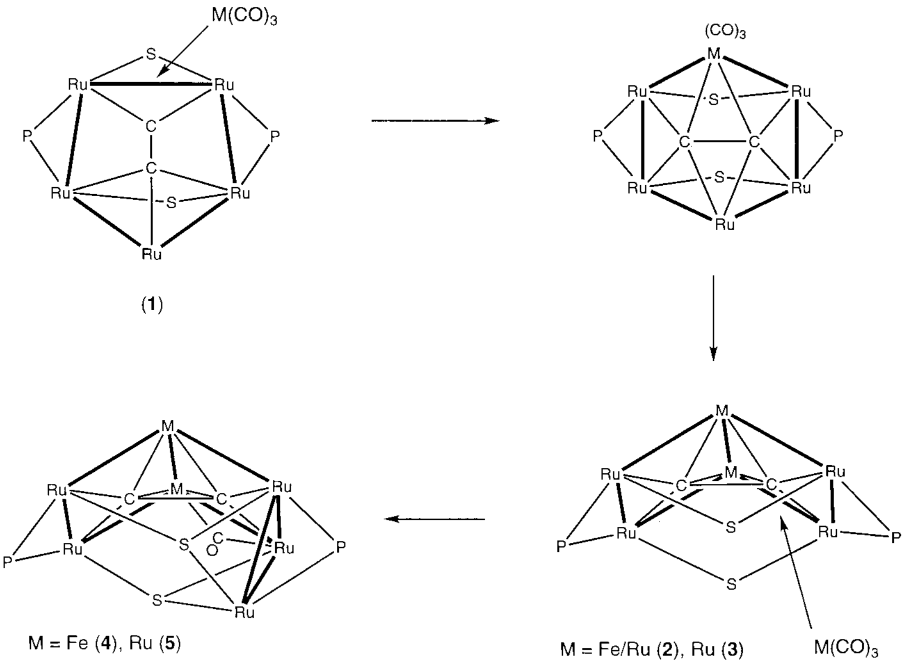

Scheme 2.

Table 2
Crystal data and refinement details for complexes **2**, **3**, **4** and **5**

Compound	**2** ($FeRu_5$)	**3** (Ru_6)	**4** (Fe_2Ru_5)	**4s** (Fe_2Ru_5)	**5** (Ru_7)
Formula	$C_{42}H_{26}FeO_{14}P_2Ru_5S_2 \cdot C_7H_8$	$C_{42}H_{26}O_{14}P_2Ru_6S_2$	$C_{44}H_{26}Fe_2O_{16}P_2Ru_5S_2. \sim 0.5C_6H_{14}$	$C_{44}H_{26}Fe_2O_{16}P_2Ru_5S_2. \sim 0.75CH_2Cl_2$	$C_{44}H_{26}O_{16}P_2Ru_7S_2$
MW	1534.1	1487.2	~ 1596.9	~ 1617.5	1664.4
Crystal system	Monoclinic	Orthorhombic	Triclinic	Monoclinic	Triclinic
Space group	$C2/c$ (No. 15)	$F2dd$ (No. 43)[a]	$P\bar{1}$ (No. 2)	$P2_1/c$ (No. 14)	$P\bar{1}$ (No. 2)
a (Å)	44.65(3)	10.685(5)	24.594(10)	19.923(9)	16.304(8)
b (Å)	11.307(6)	36.597(18)	10.971(5)	11.087(8)	14.827(12)
c (Å)	21.81(1)	48.77(2)	10.606(5)	25.221(9)	10.967(13)
α (°)			104.02(4)		89.24(5)
β (°)	102.61(5)		96.12(4)	102.31(4)	88.37(3)
γ (°)			96.38(3)		85.30(5)
V (Å^3)	10745	19062	2733	5443	2641
Z	8	16	2	4	2
D_c (g cm^{-3})	1.90	2.07	1.94	1.97	2.07
$F(000)$	5984	11456	~ 1554	~ 3134	1576
Crystal size (mm)	0.65 × 0.30 × 0.55	0.65 × 0.23 × 0.28	0.25 × 0.48 × 0.30	0.075 × 0.42 × 0.07	0.15 × 0.04 × 0.38
A^a (min, max)	1.56, 2.62	1.32, 1.45	1.50, 1.74	1.11, 1.28	1.16, 1.35
μ, cm^{-1}	17.0	20.2	18.9	19.4	19.3
$2\theta_{max}$ (°)	50	55	50	45	50
N	8881	5787	9620	7088	9322
N_0	5918	4758	6542	2652	4737
R	0.034	0.027[a]	0.036	0.10	0.050
R_w	0.031	0.027[a]	0.040	0.10	0.046

[a] Both chiralities; $F2dd$ is a nonstandard setting of $Fdd2$.

Table 3
Non-hydrogen positional and isotropic displacement parameters, (**2**)

Atom	*x*	*y*	*z*	*U*(eq) Å^2
Ru(1)	0.40612(1)	0.46101(5)	0.63837(2)	0.0344(2)
Fe(2)[a]	0.3518(2)	0.3124(8)	0.6024(3)	0.073(3)
Ru(2)[a]	0.35150(7)	0.3104(3)	0.6021(1)	0.027(1)
Ru(3)	0.33000(1)	0.45445(5)	0.69637(2)	0.0321(2)
Ru(4)	0.30315(1)	0.62245(5)	0.60087(2)	0.0307(2)
Fe(5)[a]	0.3255(3)	0.477(1)	0.5063(4)	0.039(4)
Ru(5)[a]	0.3251(1)	0.4801(7)	0.5051(2)	0.032(2)
Ru(6)	0.37979(1)	0.62826(5)	0.54069(2)	0.0321(2)
S(1)	0.38072(4)	0.5481(2)	0.71602(7)	0.0386(6)
C(01)	0.4014(2)	0.5193(8)	0.7954(3)	0.075(3)
S(2)	0.35061(4)	0.7355(1)	0.60657(7)	0.0377(6)
C(02)	0.3406(2)	0.8849(6)	0.5766(4)	0.081(4)
C(11)	0.4252(1)	0.3780(7)	0.5818(3)	0.049(3)
O(11)	0.4373(1)	0.3227(5)	0.5512(2)	0.082(3)
C(12)	0.4377(2)	0.4090(7)	0.7041(3)	0.057(3)
O(12)	0.4572(1)	0.3791(6)	0.7441(2)	0.109(3)
C(21)	0.3704(2)	0.2166(7)	0.5529(4)	0.063(3)
O(21)	0.3807(2)	0.1513(6)	0.5234(3)	0.109(3)
C(22)	0.3179(2)	0.2110(7)	0.5904(4)	0.059(3)
O(22)	0.2993(1)	0.1420(5)	0.5833(3)	0.091(3)
C(23)	0.3712(2)	0.2527(7)	0.6796(3)	0.064(3)
O(23)	0.3827(1)	0.2044(5)	0.7247(2)	0.088(3)
C(31)	0.2926(2)	0.3697(6)	0.6789(3)	0.041(3)
O(31)	0.2706(1)	0.3164(4)	0.6693(2)	0.061(2)
C(32)	0.3396(2)	0.3962(6)	0.7789(3)	0.046(3)
O(32)	0.3458(1)	0.3593(5)	0.8293(2)	0.079(2)
C(41)	0.2656(2)	0.5388(6)	0.5808(3)	0.041(2)
O(41)	0.2428(1)	0.4922(5)	0.5652(2)	0.067(2)
C(42)	0.2806(1)	0.7615(6)	0.5726(3)	0.039(2)
O(42)	0.2670(1)	0.8442(4)	0.5565(2)	0.066(2)
C(51)	0.3428(2)	0.4198(7)	0.4429(3)	0.055(3)
O(51)	0.3530(1)	0.3824(5)	0.4034(3)	0.090(3)
C(52)	0.2890(2)	0.3938(8)	0.4790(3)	0.063(3)
O(52)	0.2679(1)	0.3386(6)	0.4600(3)	0.106(3)
C(53)	0.3116(2)	0.6183(7)	0.4672(3)	0.055(3)
O(53)	0.3023(1)	0.6999(5)	0.4358(2)	0.074(2)
C(61)	0.4000(1)	0.5550(6)	0.4840(3)	0.043(3)
O(61)	0.4120(1)	0.5202(5)	0.4472(2)	0.067(2)
C(62)	0.3767(2)	0.7647(7)	0.4903(3)	0.061(3)
O(62)	0.3737(2)	0.8469(6)	0.4600(3)	0.111(3)
C(1)	0.3614(1)	0.4846(5)	0.5830(2)	0.030(2)
C(2)	0.3347(1)	0.4820(5)	0.6028(2)	0.031(2)
P(1)	0.30303(4)	0.6245(2)	0.70746(7)	0.0343(6)
C(111)	0.3191(1)	0.7422(6)	0.7622(3)	0.040(2)
C(112)	0.3040(2)	0.7798(6)	0.8090(3)	0.048(3)
C(113)	0.3176(2)	0.8629(7)	0.8530(3)	0.058(3)
C(114)	0.3450(2)	0.9093(7)	0.8512(4)	0.068(3)
C(115)	0.3602(2)	0.8773(7)	0.8051(4)	0.068(3)
C(116)	0.3474(2)	0.7920(7)	0.7612(3)	0.054(3)
C(121)	0.2658(1)	0.5997(6)	0.7275(3)	0.040(2)
C(122)	0.2642(2)	0.5287(7)	0.7792(3)	0.052(3)
C(123)	0.2369(2)	0.5098(7)	0.7955(4)	0.066(4)
C(124)	0.2105(2)	0.5622(8)	0.7611(4)	0.069(4)
C(125)	0.2117(2)	0.6320(7)	0.7112(4)	0.062(3)
C(126)	0.2397(2)	0.6516(6)	0.6940(3)	0.047(3)
P(2)	0.42565(4)	0.6379(2)	0.61340(7)	0.0364(6)
C(211)	0.4333(2)	0.7577(7)	0.6692(3)	0.054(3)
C(212)	0.4236(2)	0.8696(9)	0.6514(5)	0.100(5)
C(213)	0.4295(3)	0.965(1)	0.6921(6)	0.126(6)
C(214)	0.4445(4)	0.943(1)	0.7504(7)	0.147(9)
C(215)	0.4557(4)	0.834(1)	0.7705(5)	0.158(8)
C(216)	0.4493(3)	0.7406(9)	0.7291(4)	0.104(5)
C(221)	0.4621(1)	0.6300(6)	0.5883(3)	0.041(2)
C(222)	0.4669(2)	0.6965(7)	0.5388(3)	0.053(3)
C(223)	0.4952(2)	0.6916(7)	0.5214(3)	0.064(3)
C(224)	0.5181(2)	0.6204(8)	0.5532(3)	0.064(3)
C(225)	0.5136(2)	0.5565(8)	0.6025(4)	0.071(4)
C(226)	0.4855(2)	0.5601(7)	0.6198(3)	0.057(3)
C(101)	0.4565(5)	0.020(2)	0.9204(6)	0.140(9)
C(1011)	0.4382(5)	−0.036(2)	0.9425(8)	0.27(1)
C(102)	0.4856(3)	0.015(1)	0.9133(6)	0.107(6)
C(103)	0.4986(5)	0.094(2)	0.8841(7)	0.19(1)
C(104)	0.4892(6)	0.182(2)	0.8580(7)	0.20(1)
C(105)	0.4547(5)	0.196(1)	0.8625(6)	0.138(8)
C(106)	0.4361(4)	0.130(1)	0.8900(6)	0.135(8)

[a] Site occupancy factor = 0.5.

atom. The observations of two SMe resonances in the cases of **2** and **4** are consistent with the solid state structures being present in solution, with no fluxional processes leading to their becoming equivalent.

3.1. Electron counts

The clusters we have described above present several unusual structural features. Extensive arrays of metals atoms are held in relatively open arrangements by the C_2 and SMe ligands. Metal–metal separations of > 3.0 Å are weakly bonding at best and it is appropriate at this stage to consider the cluster valence electron (c.v.e.) counts for complexes **2–5**. Complexes **2** and **3** are 94-e clusters and their geometries can be derived from 90-e trigonal prisms by cleavage of two M–M bonds [29]; the same c.v.e. count is expected on the basis of Mingos's condensed cluster counting rules [30]. Individual metal atoms achieve 18-e configurations in all cases if the C_2 ligand is considered to be a 6-e donor.

In contrast, complexes **4** and **5** are electron-rich with 110 c.v.e., two more than expected. There are now many examples of clusters containing several 3-e bridging ligands, such as PR_2 or SR, which are formally electron-rich [31–33]. Structural studies have shown these complexes to have one or more lengthened M–M vectors (or enlarged triangular faces), a feature which has been rationalised by EH MO calculations as resulting from the extra electrons being accommodated in low-lying orbitals that have M–M antibonding character [34–36]. The several longer-than-normal M–M vectors found in **4** and **5** suggest that a similar explanation operates here.

The electron configurations of these complexes have been considered before in a survey of higher nuclearity clusters containing the C_2 ligand [29]. While the metal skeleton is related to a trigonal prism, this core is too

Table 4
Non-hydrogen positional and isotropic displacement parameters, (**3**)

Atom	x	y	z	U(eq) Å* 2
Ru(1)	0.50058(5)	0.30918(1)	0.39672(1)	0.0308(2)
Ru(2)	0.44285(6)	0.28258(1)	0.45250(1)	0.0333(2)
Ru(3)	0.60461(5)	0.34518(1)	0.46917(1)	0.0295(2)
Ru(4)	0.39098(5)	0.39336(1)	0.46991(1)	0.0290(1)
Ru(5)	0.22296(5)	0.33205(1)	0.45376(1)	0.0319(2)
Ru(6)	0.28935(5)	0.35857(1)	0.39774(1)	0.0318(2)
C(11)	0.4020(7)	0.2724(2)	0.3821(1)	0.042(2)
O(11)	0.3446(6)	0.2490(1)	0.3728(1)	0.068(2)
C(12)	0.6428(7)	0.2871(2)	0.3805(1)	0.044(2)
O(12)	0.7273(6)	0.2733(2)	0.3708(1)	0.071(2)
C(21)	0.3644(9)	0.2394(2)	0.4392(2)	0.059(3)
O(21)	0.3179(8)	0.2127(2)	0.4325(1)	0.105(3)
C(22)	0.4309(8)	0.2647(2)	0.4896(1)	0.054(3)
O(22)	0.4224(8)	0.2541(2)	0.5111(1)	0.094(3)
C(23)	0.6096(8)	0.2660(2)	0.4464(2)	0.052(3)
O(23)	0.7084(6)	0.2531(2)	0.4438(1)	0.079(2)
C(31)	0.5850(7)	0.3308(2)	0.5059(1)	0.044(2)
O(31)	0.5802(6)	0.3203(2)	0.5278(1)	0.072(2)
C(32)	0.7771(7)	0.3361(2)	0.4744(1)	0.047(3)
O(32)	0.8819(5)	0.3308(2)	0.4779(1)	0.077(2)
C(41)	0.3655(7)	0.3806(2)	0.5073(1)	0.041(2)
O(41)	0.3473(6)	0.3737(2)	0.5295(1)	0.063(2)
C(42)	0.3123(8)	0.4384(2)	0.4759(1)	0.048(3)
O(42)	0.2667(7)	0.4659(1)	0.4796(1)	0.081(3)
C(51)	0.1080(7)	0.2977(2)	0.4388(1)	0.045(2)
O(51)	0.0403(6)	0.2766(2)	0.4301(1)	0.074(2)
C(52)	0.1771(6)	0.3197(2)	0.4908(1)	0.044(2)
O(52)	0.1449(6)	0.3113(2)	0.5121(1)	0.074(2)
C(53)	0.1228(7)	0.3742(2)	0.4508(2)	0.047(3)
O(53)	0.0525(6)	0.3980(1)	0.4497(1)	0.068(2)
C(61)	0.1913(7)	0.3227(2)	0.3809(1)	0.046(3)
O(61)	0.1232(6)	0.3030(2)	0.3708(1)	0.077(2)
C(62)	0.1782(8)	0.3924(2)	0.3830(2)	0.059(3)
O(62)	0.1071(7)	0.4122(2)	0.3738(1)	0.099(3)
S(1)	0.6422(2)	0.35298(5)	0.41959(3)	0.0358(5)
C(01)	0.8066(7)	0.3428(3)	0.4123(2)	0.066(3)
S(2)	0.3986(2)	0.40870(4)	0.42107(3)	0.0359(5)
C(02)	0.3121(9)	0.4507(2)	0.4156(2)	0.058(3)
C(1)	0.3852(6)	0.3278(2)	0.4285(1)	0.028(2)
C(2)	0.4218(6)	0.3405(2)	0.4540(1)	0.029(2)
P(1)	0.5996(2)	0.40676(5)	0.47972(3)	0.0330(5)
C(111)	0.7049(7)	0.4385(2)	0.4618(1)	0.038(2)
C(112)	0.7938(8)	0.4578(2)	0.4764(1)	0.053(3)
C(113)	0.8827(8)	0.4791(2)	0.4630(2)	0.065(3)
C(114)	0.8799(9)	0.4819(2)	0.4347(2)	0.063(3)
C(115)	0.7917(9)	0.4636(2)	0.4202(2)	0.064(3)
C(116)	0.7038(8)	0.4416(2)	0.4333(1)	0.052(3)
C(121)	0.6232(7)	0.4206(2)	0.5154(1)	0.042(2)
C(122)	0.7086(7)	0.4038(2)	0.5320(1)	0.051(3)
C(123)	0.7275(8)	0.4162(2)	0.5591(2)	0.065(3)
C(124)	0.6585(9)	0.4451(3)	0.5684(2)	0.074(4)
C(125)	0.5737(9)	0.4618(2)	0.5519(2)	0.065(3)
C(126)	0.5561(8)	0.4497(2)	0.5258(2)	0.060(3)
P(2)	0.4446(2)	0.35216(5)	0.36464(3)	0.0348(5)
C(211)	0.5580(7)	0.3878(2)	0.3565(1)	0.035(2)
C(212)	0.5339(8)	0.4247(2)	0.3573(2)	0.058(3)
C(213)	0.624(1)	0.4499(2)	0.3495(2)	0.074(4)
C(214)	0.7385(9)	0.4386(2)	0.3421(2)	0.064(3)
C(215)	0.7687(9)	0.4028(2)	0.3416(2)	0.066(3)
C(216)	0.6794(8)	0.3771(2)	0.3483(1)	0.053(3)
C(221)	0.3949(7)	0.3389(2)	0.3301(1)	0.039(2)
C(222)	0.3259(7)	0.3639(2)	0.3149(1)	0.050(3)
C(223)	0.2911(8)	0.3558(3)	0.2883(2)	0.066(3)
C(224)	0.3215(8)	0.3240(2)	0.2766(2)	0.064(3)
C(225)	0.391(1)	0.2990(2)	0.2913(2)	0.064(3)
C(226)	0.4283(9)	0.3067(2)	0.3180(1)	0.056(3)

small to encapsulate the C_2 ligand, so that two M–M bonds are 'broken' (by retention of two more ligands than would be required by the trigonal prism). The relationship of the cores present in **2** and **3** to that in the heterometallic cluster $[Co_3Fe_3(\mu_3,\mu_3\text{-}C_2)(CO)_{18}]^{2-}$, which can also be related to a trigonal prism by cleavage of two (different) M–M bonds, has also been noted.

There is a strong interaction of the C_2 ligand with the resulting metal cage, comprising donation from C_2 σ(p) and π bonding frontier MOs into vacant metal MOs and back bonding from filled metal MOs to the C_2 π^* orbitals. The C_2 ligand is negatively charged (about -0.32 e on each carbon atom) with an overlap population of 1.20. It will be interesting to explore the chemistry of these complexes further, although the relatively high steric protection of the C_2 ligand suggests that it will be difficult to get it to participate in reactions.

4. Conclusions

The high reactivity of cluster **1** extends to its reactions with metal carbonyls such as $Fe_2(CO)_9$ and $Ru(CO)_5$. From these reactions, we have isolated and characterised the four complexes described above, which contain novel cluster geometries. Possible routes to these complexes have been discussed, involving attack at the cluster and rearrangement. These observations are consistent with the expected behaviour of **1** being manifested not only in chemistry of the exposed C_2 ligand (here in further interactions with metal atoms) but also at the SMe groups, which in **4** and **5**, adopt the triple-bridging bonding mode.

5. Experimental

5.1. General conditions

All reactions were carried out under dry, high purity nitrogen using standard Schlenk techniques. Solvents were dried and distilled before use. Elemental analyses were by the Canadian Microanalytical Service, Delta, BC, Canada V4G 1G7. TLC was carried out using glass plates (20 × 20 cm) coated with silica gel (Merck 60 GF_{254}, 0.5 mm thick).

Table 5
Non-hydrogen positional and isotropic displacement parameters, (**4**)

Atom	*x*	*y*	*z*	*U*(eq) Å^2
Ru(1)	0.30808(3)	0.02183(6)	0.11628(5)	0.0443(2)
Fe(2)	0.23252(4)	−0.07063(9)	−0.10077(9)	0.0404(4)
Ru(3)	0.16179(3)	0.09899(5)	0.03975(6)	0.0418(2)
Ru(4)	0.19899(3)	0.28301(5)	−0.09358(5)	0.0393(2)
Fe(5)	0.26673(4)	0.11503(9)	−0.22650(9)	0.0394(4)
Ru(6)	0.35330(3)	0.23885(5)	−0.01426(5)	0.0388(2)
Ru(7)	0.32254(3)	0.30507(5)	0.25162(5)	0.0412(2)
S(1)	0.24163(8)	0.1465(2)	0.2148(2)	0.0435(7)
C(01)	0.2235(4)	0.0997(8)	0.3586(7)	0.067(4)
S(2)	0.28428(8)	0.3702(2)	0.0589(2)	0.0394(7)
C(02)	0.3004(3)	0.5398(7)	0.0745(7)	0.057(3)
C(11)	0.3588(3)	−0.0778(7)	0.0374(7)	0.060(3)
O(11)	0.3870(3)	−0.1456(6)	−0.0091(6)	0.089(3)
C(12)	0.3271(4)	−0.0333(8)	0.2676(8)	0.076(4)
O(12)	0.3361(3)	−0.0751(7)	0.3566(6)	0.121(4)
C(21)	0.2700(3)	−0.1880(7)	−0.1917(7)	0.052(3)
O(21)	0.2908(3)	−0.2630(5)	−0.2527(6)	0.089(3)
C(22)	0.1693(3)	−0.1645(7)	−0.1764(7)	0.057(3)
O(22)	0.1305(2)	−0.2342(5)	−0.2284(6)	0.091(3)
C(23)	0.2402(3)	−0.1327(6)	0.0494(7)	0.054(3)
O(23)	0.2227(3)	−0.2094(5)	0.0999(5)	0.076(3)
C(31)	0.1011(3)	0.0361(7)	−0.0897(8)	0.057(3)
O(31)	0.0622(3)	−0.0022(5)	−0.1643(6)	0.092(3)
C(32)	0.1198(4)	0.0350(8)	0.1530(8)	0.069(4)
O(32)	0.0936(3)	−0.0037(7)	0.2208(6)	0.116(4)
C(41)	0.1446(3)	0.2121(7)	−0.2376(7)	0.058(3)
O(41)	0.1136(3)	0.1724(6)	−0.3305(6)	0.091(3)
C(42)	0.1966(3)	0.4395(7)	−0.1374(7)	0.056(3)
O(42)	0.1951(3)	0.5321(5)	−0.1678(6)	0.089(3)
C(51)	0.3239(3)	0.0494(7)	−0.2985(6)	0.052(3)
O(51)	0.3586(3)	0.0063(6)	−0.3464(5)	0.081(3)
C(52)	0.2160(3)	0.0122(7)	−0.3502(7)	0.054(3)
O(52)	0.1855(3)	−0.0535(5)	−0.4350(5)	0.078(3)
C(53)	0.2671(3)	0.2506(7)	−0.2943(7)	0.052(3)
O(53)	0.2710(3)	0.3255(5)	−0.3529(5)	0.072(3)
C(61)	0.4078(3)	0.1323(7)	−0.0477(7)	0.054(3)
O(61)	0.4437(2)	0.0754(5)	−0.0691(6)	0.075(3)
C(62)	0.3777(3)	0.3272(7)	−0.1317(7)	0.059(3)
O(62)	0.3917(3)	0.3795(6)	−0.2080(5)	0.086(3)
C(71)	0.3121(3)	0.4545(7)	0.3715(7)	0.059(3)
O(71)	0.3083(3)	0.5468(6)	0.4437(6)	0.096(3)
C(72)	0.3578(3)	0.2514(7)	0.3921(7)	0.058(3)
O(72)	0.3790(3)	0.2274(6)	0.4807(5)	0.086(3)
P(1)	0.13974(9)	0.3001(2)	0.0624(2)	0.0456(7)
C(111)	0.1572(3)	0.4208(6)	0.2174(7)	0.046(3)
C(112)	0.1677(3)	0.5476(7)	0.2170(8)	0.062(3)
C(113)	0.1790(4)	0.6420(8)	0.3338(8)	0.081(4)
C(114)	0.1784(4)	0.6094(9)	0.4495(8)	0.088(4)
C(115)	0.1678(5)	0.4851(9)	0.4509(8)	0.092(5)
C(116)	0.1576(4)	0.3906(8)	0.3366(8)	0.072(4)
C(121)	0.0684(3)	0.3131(7)	0.0174(8)	0.061(3)
C(122)	0.0305(4)	0.278(1)	0.090(1)	0.104(6)
C(123)	−0.0258(5)	0.280(1)	0.060(2)	0.145(8)
C(124)	−0.0433(4)	0.319(1)	−0.046(1)	0.135(7)
C(125)	−0.0077(5)	0.356(1)	−0.120(1)	0.125(6)
C(126)	0.0492(4)	0.3532(9)	−0.0878(9)	0.085(4)
C(1)	0.2830(3)	0.1011(5)	−0.0372(6)	0.036(2)
C(2)	0.2283(3)	0.1151(6)	−0.0673(6)	0.035(2)
P(2)	0.40532(8)	0.3616(2)	0.1813(2)	0.0436(7)
C(211)	0.4287(3)	0.5288(6)	0.1965(7)	0.048(3)
C(212)	0.4302(4)	0.6170(8)	0.3161(8)	0.073(4)
C(213)	0.4491(5)	0.7443(8)	0.3262(9)	0.097(5)
C(214)	0.4676(4)	0.7829(8)	0.223(1)	0.093(5)
C(215)	0.4669(4)	0.6948(7)	0.1059(8)	0.067(4)
C(216)	0.4472(3)	0.5702(7)	0.0929(7)	0.052(3)
C(221)	0.4696(3)	0.3132(7)	0.2417(6)	0.048(3)
C(222)	0.5197(3)	0.3940(7)	0.2670(8)	0.060(3)
C(223)	0.5688(3)	0.3558(9)	0.3089(9)	0.074(4)
C(224)	0.5695(4)	0.2379(8)	0.3257(8)	0.070(4)
C(225)	0.5202(4)	0.1565(8)	0.3015(9)	0.073(4)
C(226)	0.4709(3)	0.1925(7)	0.2593(8)	0.059(3)
C(101)[a]	−0.0428(9)	0.163(2)	0.524(2)	0.120(8)
C(102)[a]	0.002(1)	0.194(2)	0.460(3)	0.17(1)
C(103)[a]	0.0305(9)	0.336(2)	0.505(2)	0.133(9)
C(104)[a]	−0.003(1)	0.437(2)	0.503(4)	0.20(1)
C(105)[a]	0.032(1)	0.568(4)	0.525(8)	0.52(5)
C(106)[a]	0.010(1)	0.700(3)	0.505(3)	0.17(1)

[a] Site occupancy factor = 0.5.

5.2. Instrumentation

IR: Perkin-Elmer 1700X FTIR; 683 double beam, NaCl optics. NMR: Bruker CXP300 or ACP300 (^{1}H NMR at 300.13 MHz, ^{13}C NMR at 75.47 MHz). FAB MS: VG ZAB 2HF (3-nitrobenzyl alcohol as matrix, Ar as exciting gas, gun voltage 7.5 kV, current 1 mA, accelerating potential 7 kV).

5.3. Reaction of **1** with $Fe_2(CO)_9$

A mixture of $Fe_2(CO)_9$ (340 mg, 0.93 mmol) and **1** (95 mg, 0.073 mmol) was heated in toluene (10 ml) in a Carius tube at 98°C for 6 h. After removal of solvent, the residue was purified by preparative TLC (light petroleum/acetone 10/3). The main orange band (R_f 0.4) was recrystallised from CH_2Cl_2/MeOH to yield orange crystals of $FeRu_5(\mu_6\text{-}C_2)(\mu\text{-SMe})_2(\mu\text{-}PPh_2)_2(CO)_{14}$ (**2**) (89 mg, 84%). Anal. Found: C, 34.94; H, 1.88; M$^+$, 1442. $C_{42}H_{26}FeO_{14}P_2Ru_5S_2$ calc. C, 34.99; H, 1.82%; M, 1442. IR (cyclohexane): ν(CO) 2073s, 2041vs, 2034s, 2020s, 2003w, 1990m, 1977s, 1926vw cm^{-1}. ^{1}H NMR: δ($CDCl_3$) 1.87, 1.93 (2 × 3H, s, SMe), 6.90–7.83 (20H, Ph). ^{13}C NMR: δ($CDCl_3$) 18.56, 18.79 (2 × s, SMe), 127.26–132.50 (m, Ph), 139.24 (d, $J_{CP} = 20.0$ Hz, *ipso* C), 142.27 (d, $J_{CP} = 36.1$ Hz, *ipso* C), 191.03 (d, $J_{CP} = 7.0$ Hz), 191.72 (d, $J_{CP} = 6.9$ Hz), 195.56 (m, br), 196.42 (s), 200.68 (s), 201.36 (s), 212.44 (m, br) (CO), 254.93 (d, $J_{CP} = 5.4$ Hz, C_2). FAB MS (*m/z*): 1442, M$^+$; 1414–1050, [M–*n*CO]$^+$ (*n* = 1–14). A second minor brown band (R_f 0.25) was recrystallised from CH_2Cl_2/MeOH to give black crystals of $Fe_2Ru_5(\mu_6\text{-}C_2)(\mu_3\text{-SMe})_2(\mu\text{-}PPh_2)_2(\mu\text{-CO})(CO)_{15}$ (**4**) (20 mg, 17%). Anal. Found: C, 34.23; H, 1.83; M$^+$, 1554. $C_{44}H_{26}Fe_2O_{16}P_2Ru_5S_2$ calc.: C 34.46; H, 1.71%; M, 1554. IR (cyclohexane): ν(CO) 2073w, 2068s, 2043vs, 2034m, 2027s, 2004(sh), 2016m, 2004s, 1990w, 1985(sh), 1977m, 1975m, 1959w, 1949w, 1872vw cm^{-1}. ^{1}H NMR: δ($CDCl_3$)

Table 6
Non-hydrogen positional and isotropic displacement parameters, (**5**)

Atom	x	y	z	U(eq) Å* 2
Ru(1)	0.75018(8)	0.82912(8)	0.6123(1)	0.0297(4)
Ru(2)	0.81913(8)	0.65043(9)	0.5897(1)	0.0336(5)
Ru(3)	0.68366(8)	0.63375(8)	0.4171(1)	0.0325(5)
Ru(4)	0.78398(8)	0.68127(8)	0.2142(1)	0.0284(4)
Ru(5)	0.92458(8)	0.69511(9)	0.3712(1)	0.0338(5)
Ru(6)	0.85935(8)	0.88730(8)	0.3874(1)	0.0291(4)
Ru(7)	0.67781(7)	0.93074(8)	0.3939(1)	0.0281(4)
S(1)	0.6400(2)	0.7901(3)	0.4836(3)	0.032(1)
C(01)	0.5421(9)	0.798(1)	0.566(1)	0.049(6)
S(2)	0.7619(2)	0.8456(2)	0.2411(3)	0.029(1)
C(02)	0.766(1)	0.904(1)	0.096(1)	0.041(6)
C(11)	0.834(1)	0.858(1)	0.715(1)	0.039(6)
O(11)	0.8784(8)	0.8746(8)	0.789(1)	0.070(6)
C(12)	0.6798(9)	0.893(1)	0.724(2)	0.043(6)
O(12)	0.6401(8)	0.9295(9)	0.801(1)	0.079(6)
C(21)	0.904(1)	0.656(1)	0.705(1)	0.050(7)
O(21)	0.9563(8)	0.659(1)	0.773(1)	0.091(7)
C(22)	0.814(1)	0.531(1)	0.625(2)	0.066(8)
O(22)	0.813(1)	0.456(1)	0.655(1)	0.119(9)
C(23)	0.7313(9)	0.702(1)	0.702(1)	0.036(6)
O(23)	0.6849(7)	0.6839(8)	0.782(1)	0.063(5)
C(31)	0.720(1)	0.511(1)	0.397(1)	0.056(8)
O(31)	0.737(1)	0.4363(8)	0.387(1)	0.086(7)
C(32)	0.591(1)	0.597(1)	0.505(2)	0.068(8)
O(32)	0.537(1)	0.575(1)	0.561(1)	0.133(9)
C(41)	0.821(1)	0.560(1)	0.185(1)	0.041(6)
O(41)	0.8450(8)	0.4866(8)	0.158(1)	0.076(6)
C(42)	0.809(1)	0.703(1)	0.048(1)	0.042(6)
O(42)	0.8263(9)	0.7183(9)	−0.051(1)	0.077(6)
C(51)	1.016(1)	0.716(1)	0.474(1)	0.047(7)
O(51)	1.0702(8)	0.7251(9)	0.532(1)	0.082(6)
C(52)	0.950(1)	0.567(1)	0.373(1)	0.047(7)
O(52)	0.9639(8)	0.4911(8)	0.377(1)	0.077(6)
C(53)	0.978(1)	0.711(1)	0.216(2)	0.062(8)
O(53)	1.0114(9)	0.721(1)	0.122(1)	0.101(7)
C(61)	0.932(1)	0.911(1)	0.508(1)	0.043(6)
O(61)	0.9827(7)	0.9226(8)	0.578(1)	0.062(5)
C(62)	0.937(1)	0.914(1)	0.268(2)	0.055(7)
O(62)	0.9824(8)	0.9317(9)	0.190(1)	0.081(6)
C(71)	0.605(1)	0.975(1)	0.281(1)	0.037(6)
O(71)	0.5577(7)	1.0048(8)	0.211(1)	0.064(5)
C(72)	0.6196(9)	1.000(1)	0.513(1)	0.040(6)
O(72)	0.5811(7)	1.0479(8)	0.577(1)	0.060(5)
P(1)	0.6481(2)	0.6492(3)	0.2151(4)	0.033(1)
C(111)	0.5697(9)	0.7339(9)	0.161(1)	0.032(5)
C(112)	0.576(1)	0.774(1)	0.049(1)	0.048(7)
C(113)	0.515(1)	0.835(1)	0.006(2)	0.064(8)
C(114)	0.446(1)	0.858(1)	0.079(2)	0.067(8)
C(115)	0.438(1)	0.819(1)	0.193(2)	0.065(8)
C(116)	0.499(1)	0.757(1)	0.234(1)	0.043(6)
C(121)	0.623(1)	0.5485(9)	0.134(1)	0.038(6)
C(122)	0.572(1)	0.491(1)	0.185(1)	0.055(7)
C(123)	0.550(1)	0.413(1)	0.125(2)	0.076(9)
C(124)	0.585(1)	0.398(1)	0.009(2)	0.062(8)
C(125)	0.634(1)	0.453(1)	−0.044(2)	0.072(9)
C(126)	0.656(1)	0.531(1)	0.015(2)	0.057(7)
C(1)	0.8203(9)	0.7678(9)	0.463(1)	0.036(6)
C(2)	0.7957(8)	0.6931(9)	0.407(1)	0.027(5)
P(2)	0.7817(2)	1.0287(3)	0.3808(3)	0.033(1)
C(211)	0.793(1)	1.1052(9)	0.253(1)	0.039(6)
C(212)	0.726(1)	1.143(1)	0.184(2)	0.055(7)
C(213)	0.736(1)	1.209(1)	0.096(2)	0.078(9)
C(214)	0.812(2)	1.234(1)	0.069(2)	0.09(1)
C(215)	0.878(1)	1.197(2)	0.129(2)	0.083(9)
C(216)	0.871(1)	1.131(1)	0.220(2)	0.064(8)
C(221)	0.781(1)	1.110(1)	0.508(1)	0.041(6)
C(222)	0.744(1)	1.199(1)	0.491(2)	0.063(8)
C(223)	0.739(1)	1.256(1)	0.590(2)	0.075(9)
C(224)	0.773(1)	1.231(1)	0.700(2)	0.058(8)
C(225)	0.808(1)	1.148(1)	0.713(2)	0.065(8)
C(226)	0.812(1)	1.084(1)	0.618(2)	0.061(8)

1.70, 2.85 (2×3H, s, SMe), 7.14–7.95 (20H, m, Ph). FAB MS (m/z): 1534, M$^+$; 1526–1106, [M–nCO]$^+$ ($n = 1$–16).

*5.4. Reaction of **1** with Ru(CO)$_5$*

Complex **1** (50 mg, 0.038 mmol) was added to a solution of Ru(CO)$_5$ [ca. 0.2 mmol; prepared from Ru$_3$(CO)$_{12}$ (50 mg, 0.078 mmol) and CO (45 atm.) in cyclohexane (20 ml) at 120°C], and the mixture was heated at 98°C for 6 h in a Carius tube. After removal of solvent, the residue was purified by preparative TLC (light petroleum/acetone 10/3). The main orange band (R_f 0.4) was recrystallised from CH$_2$Cl$_2$/MeOH to give orange crystals of Ru$_6$(μ_6-C$_2$)(μ-SMe)$_2$(μ-PPh$_2$)$_2$(CO)$_{14}$ (**3**) (48 mg, 86%). Anal. Found: C, 33.88; H, 1.77; M$^+$, 1459. C$_{42}$H$_{26}$O$_{14}$P$_2$Ru$_6$S$_2$ calc.: C, 33.87; H, 1.74%; M, 1488. IR (cyclohexane); υ(CO) 2075s, 2041vs, 2037s, 2026w, 2011m, 1991m, 1978m, 1955vw cm^{-1}. ^{1}H NMR: δ(CDCl$_3$) 1.78 (6H, s, $2 \times$ SMe), 6.79–7.82 (20H, m, Ph). ^{13}C NMR: δ(CDCl$_3$) 18.69 (s, $2 \times$ SMe), 127.21–132.71 (m, Ph), 139.26 (d, $J_{CP} = 19.6$ Hz, *ipso* C), 142.36 (d, $J_{CP} = 36.7$ Hz, *ipso* C), 191.72 (d, $J_{CP} = 7.0$ Hz), 195.77 (s, br), 196.17 (s), 201.62 (s), (CO), 252.19 (d, $J_{CP} = 8.6$ Hz, C$_2$). FAB MS (m/z): 1459–1067, [M–nCO]$^+$ ($n = 1$–14); M$^+$ not observed. A second minor orange band (R_f 0.2) was recrystallised from CH$_2$Cl$_2$/MeOH to give orange crystals of Ru$_7$(μ_6-C$_2$)(μ_3-SMe)$_2$(μ-PPh$_2$)$_2$(μ-CO)(CO)$_{15}$ (**5**) (6 mg, 10%). Anal. Found: C, 32.04; H, 1.63; M$^+$, 1644. C$_{44}$H$_{26}$O$_{16}$P$_2$Ru$_7$S$_2$ calc.: C, 32.14; H, 1.59%; M, 1644. IR (cyclohexane): υ(CO) 2072s, 2043vs, 2034s, 2024s, 2014m, 1999m, 1994m, 1974m, 1969w, 1962w, 1954w, 1820w cm^{-1}. ^{1}H NMR: δ(CDCl$_3$) 1.58 (3H, s, SMe), 2.79 (3H, d, $J_{HP} = 0.2$ Hz, SMe), 7.14–7.94 (20H, m, Ph). FAB MS (m/z): 1644, M$^+$; 1616–1196, [M–nCO]$^+$ ($n = 1$–16).

5.5. Crystallography

Unique data sets were measured at ca. 295 K within the specified $2\theta_{max}$ limits using an Enraf-Nonius CAD4 diffractometer ($2\theta/\theta$ scan mode; monochromatic Mo–Kα radiation, λ 0.7107$_3$ Å); N independent reflections were obtained N_o with $I > 3\sigma(I)$ being considered observed and used in the full matrix least squares refinement after gaussian absorption correction. Anisotropic thermal parameters were refined for the non-hydrogen atoms; $(x, y, z, U_{iso})_H$ were included constrained at estimated values. Conventional residuals R, R' on $|F|$ are quoted, statistical weights derivative of $\sigma^2(I) = \sigma^2(I_{diff}) + 0.0004\sigma^4(I_{diff})$ being used. Computation used the XTAL 3.2 program system [37] implemented by S.R. Hall; neutral atom complex scattering factors were employed. Crystal data and refinement details are given in Table 2.

5.6. Abnormal features and variations in procedure

2. This material was found to decompose in the X-ray beam; data were collected on the largest possible specimen overnight at maximum speed with periodic reorientation checks. Decomposition of about 20% was compensated for by scaling. Following exploratory refinements with variable site occupancies, the sites of Ru(2,5) were set at 50% occupancy with iron atoms; although separate components at each site were refinable in a stable manner with meaningful anisotropic thermal parameters, the separation of components at each site is small [sites 2,5: 0.03(1), 0.04(1) Å] and differences in associated geometries are of doubtful meaning and significance (Table 3; see also Table 4 for data on **3**).

4. This complex was initially isolated as inferior material as a dichloromethane solvate, **4s**, offering limited and weak data capable of supporting meaningful anisotropic thermal parameter refinement for Ru, Fe only, and with solvent population refining to 0.75. Crystallisation from hexane afforded better crystals in a different form, permitting normal refinement, the solvent being modelled/refined with constrained geometry and site occupancy 0.5. We give the results of the latter in detail; details of the dichloromethane solvent other than immediate crystal data are deposited (Table 5).

5. A satisfactory specimen was obtained only with difficulty, the crystals appearing to craze on standing, although seemingly stable in the X-ray beam (Table 6).

Acknowledgements

We thank the Australian Research council for support of this work and Johnson Matthey Technology for a generous loan of $RuCl_3 \cdot nH_2O$.

References

[1] A.M. Giroud-Godquin and P.M. Maitlis, Angew. Chem., 103 (1991) 370; Angew. Chem., Int. Ed. Engl., 30 (1991) 375.

[2] D.W. Bruce and D. O'Hare (Eds.), Inorg. Materials, Wiley: Chichester, 1992.

[3] P. Wisian-Mielson, H.R. Allcock and K.J. Wynne (Eds.), Inorganic and Organometallic Polymers II: Advanced Materials and Intermediates, ACS Symp. Ser. 572, ACS: Washington, 1994.

[4] N.J. Long, Angew. Chem., 107 (1995) 37; Angew. Chem., Int. Ed. Engl., 34 (1995) 21.

[5] J.S. Schumm, D.L. Pearson and J.M. Tour, Angew. Chem., 106 (1994) 1445; Angew. Chem., Int. Ed. Engl., 33 (1994) 1360.

[6] F. Diederich and Y. Rubin, Angew. Chem., 104 (1992) 1123; Angew. Chem., Int. Ed. Engl., 31 (1992) 1101.

[7] W. Beck, B. Niemer and M. Wieser, Angew. Chem., 105 (1993) 969; Angew. Chem., Int. Ed. Engl., 32 (1993) 923.

[8] H. Lang, Angew. Chem., 106 (1994) 569; Angew. Chem., Int. Ed. Engl., 33 (1994) 547.

[9] T. Bartik, B. Bartik, M. Brady, R. Dembinski and J.A. Gladysz, Angew. Chem., 108 (1996) 467; Angew. Chem., Int. Ed. Engl., 35 (1996) 414.

[10] A. Arrigoni, A. Ceriotti, R. Della Pergola, M. Manassero, N. Masciocchi and M. Sansoni, Angew. Chem., 96 (1984) 290; Angew. Chem., Int. Ed. Engl., 23 (1984) 322.

[11] A. Ceriotti, G. Longoni, M. Manassero, N. Masciocchi, L. Resconi and M. Sansoni, J. Chem. Soc., Chem. Commun., (1985) 181.

[12] G. Longoni, A. Ceriotti, R. Della Pergola, M. Manassero, M. Peregno, G. Piro, M. Sansoni, Phil. Trans. R. Soc. London, Ser. A 308 (1982) 47.

[13] V.G. Albano, P. Chini, S. Martinengo, M. Sansoni and D. Strumolo, J. Chem. Soc., Dalton Trans., (1978) 459.

[14] G. Bor, L. Marko, B. Marko, Chem. Ber. 95 (1962) 333.

[15] G. Allegra, E.M. Peronaci and R. Ercoli, Chem. Commun., (1966) 549.

[16] M.D. Brice, B.R. Penfold, Inorg. Chem. 11 (1972) 1381.

[17] U. Geiser, A.M. Kini, Acta Crystallogr. C49 (1993) 1322.

[18] M.P. Jensen, D.A. Phillips, M. Sabat, D.F. Shriver, Organometallics 11 (1992) 1859.

[19] G. Gervasio, R. Rosssetti, P.L. Stanghellini, G. Bor, Inorg. Chem. 23 (1984) 2073.

[20] M. Akita, H. Hirakawa, M. Tanaka, Y. Moro-oka, J. Organomet. Chem. 485 (1995) C14.

[21] M. Akita, S. Sugamoto, M. Tanaka, Y. Moro-oka, J. Am. Chem. Soc. 114 (1992) 7581.

[22] C.J. Adams, M.I. Bruce, B.W. Skelton and A.H. White, J. Chem. Soc., Chem. Commun., (1992) 26.

[23] M.I. Bruce, Coord. Chem. Rev., in press.

[24] M.I. Bruce, J. Cluster Sci. 8 (1997) 293.

[25] C.J. Adams, M.I. Bruce, B.W. Skelton and A.H. White, J. Chem. Soc., Chem. Commun., (1993) 446.

[26] E.H. Braye, L.F. Dahl, W. Hubel, D.L. Wampler, J. Am. Chem. Soc. 84 (1962) 4633.

[27] B.F.G. Johnson, J. Lewis, J.N. Nicholls, J. Puga, P.R. Raithby, M.J. Rosales, M. McPartlin and W. Clegg, J. Chem. Soc., Dalton Trans., (1983) 277.

[28] G. Frapper, J.-F. Halet, Organometallics 14 (1995) 5044.

[29] G. Frapper, J.-F. Halet, M.I. Bruce, Organometallics 16 (1997) .

[30] D.M.P. Mingos and D.J. Wales, Introduction to Cluster Chemistry, Prentice-Hall, Englewood Cliffs, 1990.

[31] G. Hogarth, J.A. Phillips, F. van Gastel, N.J. Taylor, T.B. Marder and A.J. Carty, J. Chem. Soc., Chem. Commun., (1988) 1570.

[32] J.F. Corrigan, S. Doherty, N.J. Taylor, A.J. Carty, J. Am. Chem. Soc. 114 (1992) 7557.

[33] J.F. Corrigan, S. Doherty, N.J. Taylor, A.J. Carty, Organometallics 12 (1993) 993.

[34] C. Mealli, D.M. Proserpio, J. Am. Chem. Soc. 112 (1990) 5484.

[35] N. Lugan, P.-L. Fabre, D. de Montauzon, G. Lavigne, J.-J. Bonnet, J.-Y. Saillard, J.-F. Halet, Inorg. Chem. 32 (1993) 1363.

[36] C.J. Adams, M.I. Bruce, B.W. Skelton, A.H. White, G. Frapper, J.-F. Halet, J. Chem. Soc., Dalton Trans., (1997) 371.

[37] S.R. Hall, H.D. Flack, J.M. Stewart (Eds.), 'The XTAL 3.2 User's Manual', Universities of Western Australia, Geneva and Maryland, 1992.